THE JOURNAL OF CHEMICAL PHYSICS **149**, 044507 (2018)

Reorientation kinetics of hydroxyl groups in anatase TiO_2

I. Chaplygin,[1,a)] F. Herklotz,[1] and E. V. Lavrov[1,2]
[1]*Technische Universität Dresden, 01062 Dresden, Germany*
[2]*Tomsk State University, 634050 Tomsk, Russia*

(Received 9 May 2018; accepted 17 July 2018; published online 30 July 2018)

The reorientation kinetics of hydrogen in a variety of complexes in the anatase polymorph of TiO_2 was investigated by means of stress-induced dichroism. For the hydrogen-defect resulting in an O-H vibrational mode with a frequency of 3389 cm^{-1}, the energy barrier separating adjacent equivalent in-plane sites of hydrogen was determined to be independent of the isotope and equal to 0.74 ± 0.02 eV, whereas the attempt frequency was found to be $(1.10 \pm 0.20) \times 10^{12}$ and $(0.75 \pm 0.15) \times 10^{12}$ s^{-1} for hydrogen and deuterium, respectively. The defect with vibrational modes at 3412 and 3417 cm^{-1} previously assigned to isolated hydrogen did not reveal alignment under the stress up to room temperature, which indicates that the barrier of hydrogen motion is above 0.9 eV. *Published by AIP Publishing.* https://doi.org/10.1063/1.5039584

I. INTRODUCTION

Titanium dioxide (TiO_2) also known as titania is a wide bandgap semiconductor with properties of both technological and fundamental interest.[1] It occurs in nature in three crystalline modifications: rutile, anatase, and brookite. For a variety of semiconductor applications, anatase is the material of choice since it has longer carrier lifetime,[2] exciton diffusion length,[3] and higher electron mobility.[4] More importantly, anatase reveals photocatalytic activity which is an order of magnitude higher than that of rutile.[5,6] Titania has various advantages: non-toxicity, high reactivity, and excellent stability in diverse environments. However, a problem to be resolved is that the efficiency of the photosplitting of water into hydrogen and oxygen is poor. To manufacture efficient photocatalytic devices, the photocatalytic TiO_2 should respond to visible light, which is about 45% of incident solar energy. Due to the wide bandgap of 3.2 eV, anatase, however, harvests only a small fraction of the solar energy. A step forward was achieved recently via engineering "black" hydrogenated anatase with a narrow bandgap of 1.54 eV, due to a blue-shifted valence band edge.[7]

In spite of this success, understanding of hydrogen properties in anatase TiO_2 remains limited. Hydrogen is an ubiquitous impurity in many solids and particularly in oxides. It strongly affects the electronic and structural properties of these materials. Interstitial hydrogen can act either as an amphoteric impurity, giving rise to deep gap levels with positive, neutral, and negative charge states, or it can form a shallow level at the conduction band edge and act as a donor.[8–10]

Theory predicts interstitial hydrogen forming a hydroxyl ion with the direction of the O–H bond pointing nearly along the $a(b)$ axis.[11] The hydrogen impurity level is located above the conduction-band minimum, implying that it acts as a shallow donor.[12]

Experimental studies on hydrogen in anatase are scarce and deal mostly with nano-sized materials.[13,14] Recently hydrogen-related defects were studied by means of IR absorption in natural bulk crystals.[15,16] A group of lines were observed in as-received materials and assigned to the stretch local vibrational modes (LVMs) of the hydroxyl groups. Hydrogenation from H_2 ambient at 450 °C was found to enhance those signals and give rise to IR absorption peaks at 3412 and 3417 cm^{-1} which were associated with LVMs due to the different charge states of interstitial hydrogen.

Important characteristics of any defect are the activation energy of dissociation or transition into another equivalent state. Dissociation can be followed by the formation of an identical defect but in a different lattice position, resulting in the diffusion of the species. If the thermal excitation is insufficient for breaking up a chemical bond, it may result in its reorientation, i.e., transition between equivalent positions in the crystalline lattice. For observation of reorientation, the symmetry between the states has to be broken to achieve their non-equilibrium occupation.

Stress-induced dichroism is the method of choice to address such issues. It was successfully applied to probe defects in Si,[17–20] GaAs,[21,22] ZnO,[23,24] In_2O_3,[25] and very recently to interstitial hydrogen in rutile TiO_2,[26] resulting in a great deal of insight into the kinetics of hydrogen motion in these semiconductors. Here, this technique is applied to probe the motion of hydrogen in natural anatase TiO_2 crystals. The observed stress-induced alignment and subsequent thermalization have enabled us to determine the activation energy of reorientation for the prominent hydrogen-related defect with an IR absorption line at 3389 cm^{-1}.

II. EXPERIMENTAL PROCEDURE

The sample employed in this study was a (001)-plane cut natural single crystal provided by SurfaceNet GmbH. It had

[a)]igor.chaplygin@tu-dresden.de

dimensions of about $5 \times 2 \times 0.5$ mm^3. Hydrogen and deuterium were introduced via a thermal treatment in a closed quartz ampule filled with a 1:1 mixture of H_2 and D_2 (a pressure of 0.5 bar at room temperature). The treatment was performed at 600 °C for 1 h and was terminated by quenching the ampule to room temperature in water.

Infrared absorption spectra were recorded with a Bomem DA3.01 Fourier transform spectrometer equipped with a globar light source, a KBr beamsplitter, and a liquid-nitrogen-cooled InSb detector. The spectral resolution was 0.5–1.0 cm^{-1}. The wavevector $\boldsymbol{k}$ was directed parallel to the [001] axis. Polarized light was supplied by a wire-grid polarizer with a KRS-5 substrate.

Uniaxial stress measurements with stress directed along the [100] crystallographic axis of the sample were carried out with a home-built stress rig mounted in the flow cryostat equipped with ZnSe windows. The stress was supplied via a push rod by a pneumatic cylinder. More details about the FTIR setup and the uniaxial stress rig can be found elsewhere.[15,16,23]

III. RESULTS AND DISCUSSION

A. Effect of uniaxial stress

Figure 1 shows the IR absorption spectra of the anatase TiO_2 sample treated in an H_2 + D_2 ambient at 600 °C. A number of absorption lines related to stretching vibrational modes of hydrogen or deuterium bound to oxygen are seen in the spectra. All features experience significant broadening when the sample temperature is increased from 10 K (blue) to 150 K (red). While the absorption lines at 3412 and 3417 cm^{-1} (not shown) have been associated with the neutral and positive charge states of the interstitial hydrogen donor,[15,16] respectively, the microscopic nature of the other lines remains largely unknown. In the present study, we particularly focus on the dominant hydrogen-related feature at 3389.3 cm^{-1} and its deuterium counterpart at 2512.4 cm^{-1}. Since the sample employed in our study was an (001)-plane cut wafer, we do not exclude that some defects with O–H bonds aligned parallel to $\boldsymbol{c}$ are also present in our sample and have escaped observation due to their orientation. For the issues addressed in this study, this circumstance, however, is of no importance.

Figure 2 (bottom panel) presents the sections of the polarized IR absorption spectra of the same sample subjected to a uniaxial stress of 0.31 GPa parallel to the [100] axis. The stress results in a splitting of the 3389 and 2512 cm^{-1} modes into two components each of which fully polarized either parallel or perpendicular to the stress. The top panel in the figure shows the frequency position of the split-off components as a function of stress.

In linear approximation (Hooke's law), the frequency of a nongenerate LVM shifts with a stress σ_{ik} as

$$\Delta\omega = \sum_{i,k} A_{ik}\sigma_{ik}, \tag{1}$$

where A_{ik} is the stress tensor of the defect. Since the two split-off components of the 3389 and 2512 cm^{-1} lines are polarized either parallel or perpendicular to the stress, we conclude that two of the three main axes of the stress tensor should lie in the (001) plane and be aligned parallel and perpendicular to the O–H (O–D) bond. The corresponding frequency shifts are reduced to

$$\Delta\omega_{\parallel} = A_{\parallel}\sigma, \quad \Delta\omega_{\perp} = A_{\perp}\sigma. \tag{2}$$

Table I provides the best-fit values of $A_{\parallel}$ and $A_{\perp}$ for both isotopes. The stress response of the defect assigned to

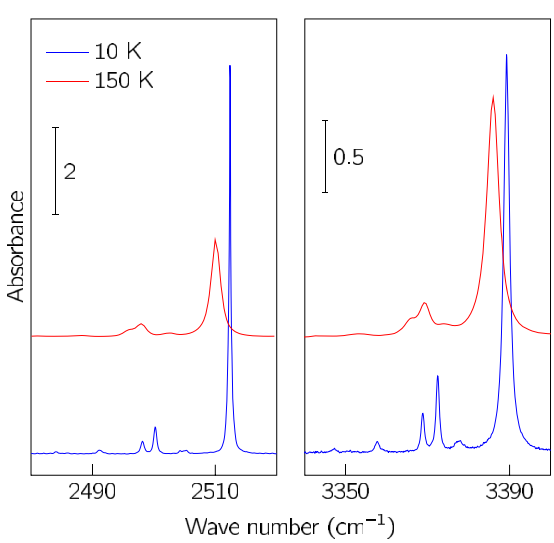

FIG. 1. Sections of the IR absorption spectra recorded at $T \leq 10$ K (blue) and 150 K (red) without stress for an anatase TiO_2 sample treated in an H_2 + D_2 ambient at 600 °C. The spectra are vertically offset for clarity.

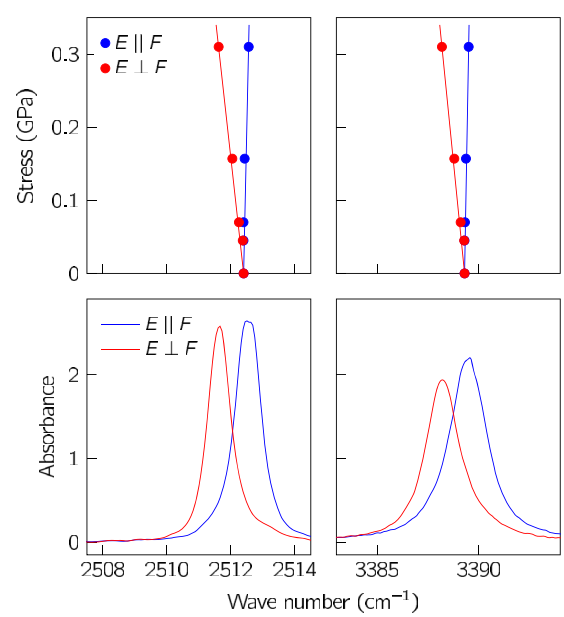

FIG. 2. Top: Split patterns of the 3389.3 cm^{-1} line (right) and its deuterium counterpart at 2512.4 cm^{-1} (left) under uniaxial stress applied perpendicular to the c axis of the anatase TiO_2 crystal. Solid lines are best-fit curves of the frequency shifts (see also the parameters given in Table I). Bottom: Exemplary IR absorption spectra taken at $T \leq 10$ K under the stress of 0.31 GPa. Blue and red stand for the polarizer aligned parallel and perpendicular to the direction of stress, respectively.

TABLE I. Piezospectroscopic coefficients $A_{\parallel}$ and $A_{\perp}$ of the 3389- and 2512-cm^{-1} lines. The indices " $\parallel$" and " $\perp$" stand for the orientation relative to the stress.

Line (cm^{-1})	$A_{\parallel}$ (cm^{-1}/GPa)	$A_{\perp}$ (cm^{-1}/GPa)
3389.3	0.6	−3.4
2512.4	0.5	−2.3

interstitial hydrogen in anatase TiO_2 is very similar to that of the 3389 cm^{-1} defect. Interestingly, the values of the stress tensor have the same order of magnitude as those reported for hydrogen-related defects in ZnO[24,27,28] but are at least a factor of ten smaller than those observed for interstitial hydrogen in rutile TiO_2.[26] Taking into account that bulk moduli of both polymorphs are around 200 GPa,[29,30] we suggest that the stress response of the hydrogen-related LVMs in both materials is determined by the microscopic structure of the defect rather than the elastic properties of the crystal.

B. Stress-induced alignment

In order to get insight into the kinetics of hydrogen motion in anatase TiO_2, we applied a two-step sequence method of stress-induced dichroism measurements. In the first step ("alignment"), a non-equilibrium occupation of hydroxyl groups is achieved by stress-induced defect alignment at elevated temperature. In the second step ("thermalization"), the reorientation process of the hydroxyl groups back to thermal equilibrium is probed by measuring the occupation distribution in a series of subsequent anneals with released stress.

Figure 3 shows the polarized absorption spectra after the anatase sample was subjected to a uniaxial stress of 0.3 GPa at 265 K for 30 min ("alignment") and subsequently cooled down to 150 K with the stress on. The spectra were recorded after the stress was released. The chosen measurement temperature of 150 K is low enough to avoid thermalization of the hydroxyl groups back to equilibrium. On the other hand, it is high enough to reduce uncertainties caused by a non-linear response of the InSb detector since the intensities of the 3389 (2512) cm^{-1} lines become significantly stronger at $T \leq 150$ K. As can be seen from the figure, the "alignment" procedure results in a redistribution of the total intensity between defects aligned parallel $I_{\parallel}$ and perpendicular $I_{\perp}$ to the stress, whereby $I_{\parallel} > I_{\perp}$. The sum of both components $I_{\parallel} + I_{\perp}$, however, remains unchanged which strongly indicates that the applied stress does not lead to dissociation of the O–H defect or its reorientation along the ***c*** axis.

Figure 4 shows the reorientation process of the defects back to the thermal equilibrium in the course of the incremental annealing treatments. After each annealing step, the sample was cooled down to 150 K in order to record new absorption spectra which were compared with the reference one. The bottom panel presents the temperature as a function of time, whereas the upper panel shows the normalized intensity differences $I_{\parallel} - I_{\perp}$ of the two components of the 3389 and 2512 cm^{-1} lines. The initial population ratio after the defect alignment $n_{\parallel}/n_{\perp} \approx 1.26$ turned out to be independent of the isotope. On the other hand, the time needed to reach the equilibrium population ratio between different orientations of the hydroxyl groups was clearly longer for the heavier isotope.

Assuming the intensities for different polarizations being proportional to the population of the correspondingly oriented state, the experimental data were fitted with the expression

$$\frac{I_{\parallel}(t) - I_{\perp}(t)}{I_{\parallel}(0) - I_{\perp}(0)} = e^{-\int_0^t \lambda(\tau)\,d\tau} \tag{3}$$

taking into account the actual temperature variation during the experiment. The details of derivation are given in Appendix A.

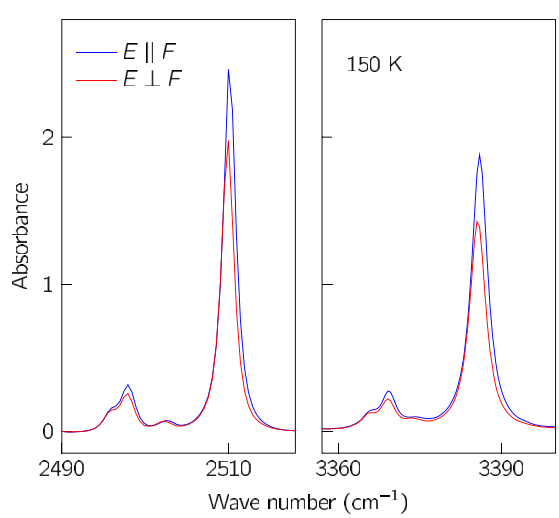

FIG. 3. Sections of the polarized IR absorption spectra of the anatase TiO_2 sample taken at 150 K after annealing the sample under the stress of 0.3 GPa at 265 K. The spectra were recorded after the stress was released.

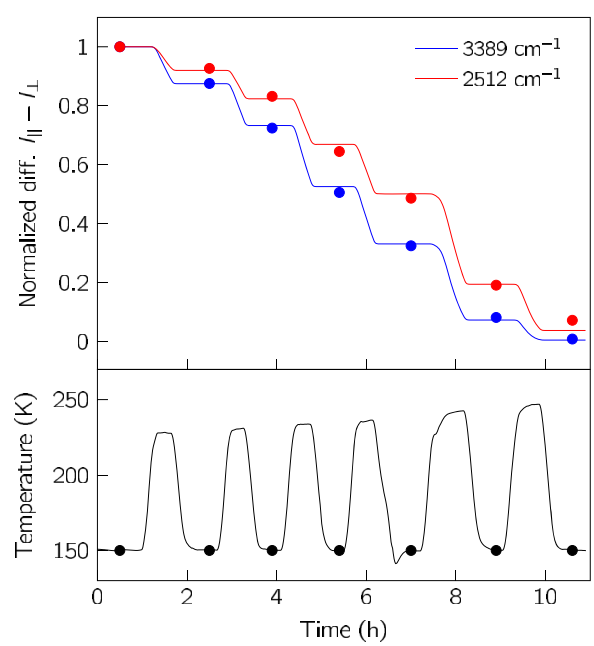

FIG. 4. Top panel: Normalized intensity differences $I_{\parallel} - I_{\perp}$ of the 3389 and 2512 cm^{-1} lines as a function of time during the process of thermalization. Solid lines are the best-fit curves (see the text). Bottom panel: Corresponding temperature vs. time. Circles indicate points at which IR absorption spectra were recorded.

The relaxation rate was modeled by the expression

$$\lambda(t) = 2\nu e^{-E/kT(t)}, \tag{4}$$

where both the attempt rate ν and the activation energy E were fitted for both hydrogen isotopes separately.

The analysis of experimental results has shown that the activation energy of the reorientation process presented in Fig. 4 is independent of the isotope. In the framework of transition state theory,[31,32] this corresponds to the high temperature classical limit.[26,33] In this limit, the attempt rate ν is independent of the temperature but depends on the isotope. Therefore in the final fit it was considered as a free parameter instead of fixing it to the quantum-mechanical limit value $\nu = kT/h$.

With this approach, one obtains the values $E_H = 0.74 \pm 0.02$ eV and $\nu_H = (1.10 \pm 0.20) \times 10^{12}$ s^{-1} for hydrogen and $E_D = 0.74 \pm 0.02$ eV and $\nu_D = (0.75 \pm 0.15) \times 10^{12}$ s^{-1} for deuterium.

Similar reorientation kinetics is observed for the complex(es) giving rise to the LVMs at 3369 and 3372 cm^{-1} (see Figs. 1 and 3). On the other hand, the defect giving rise to the 3412 and 3417 cm^{-1} IR absorption lines which was associated with an interstitial hydrogen[15,16] did not reveal alignment with uniaxial stress up to 265 K. This might indicate that the energy barrier separating equivalent sites for hydrogen in the anatase lattice is higher than that of the defect considered above. Alternatively, it might also imply that the effective attempt frequency for interstitial hydrogen is significantly lower for the anatase polymorph since the distance separating two equivalent but orthogonal to each other sites is larger than the one in rutile TiO_2. Further experiments are under way to address the issue of interstitial hydrogen diffusion and identification of other defects in anatase. In this connection, a theoretical characterization of possible hydrogen-related defects in anatase including their dissociation and reorientation energies would be of great importance.

IV. SUMMARY

In summary, the motion of hydroxyl groups in the anatase polymorph of TiO_2 was probed by means of stress induced dichroism. It was found that the activation energy of reorientation is independent of the isotope for the hydrogen-related defect with its local vibrational mode at 3389.3 cm^{-1}, suggesting the classical mechanism of this process.

ACKNOWLEDGMENTS

This work was funded by the Deutsche Forschungsgemeinschaft (Grant No. LA 1397/13). E.V.L. acknowledges the support by the Tomsk State University competitiveness improvement program (Project No. 8.2.22.2018).

APPENDIX: TWO STATE KINETIC MODEL WITH TEMPERATURE DEPENDENT TRANSITION RATE

Let N_1 and N_2 be the populations of two energy levels separated by energy Δ. The transition to equilibrium state will obey

$$\frac{d}{dt}\begin{pmatrix} N_1 \\ N_2 \end{pmatrix} = \begin{pmatrix} -r_1 & r_2 \\ r_1 & -r_2 \end{pmatrix}\begin{pmatrix} N_1 \\ N_2 \end{pmatrix}, \tag{A1}$$

where the transition rates r_1 and r_2 are assumed to be time-dependent.

Equation (A1) implies $N_1 + N_2 \equiv N = \text{const}$. Introducing $n = N_1/N$, the system (A1) can be rewritten as a single differential equation

$$\frac{dn_1}{dt} = -r_1 n_1 + r_2(1 - n_1) = -(r_1 + r_2)n_1 + r_2 \equiv -\lambda n_1 + r_2,$$

whose general solution can be obtained by ansatz

$$\begin{aligned} n(t) &= C(t)\exp\left(-\int_0^t \lambda(t')dt'\right) \equiv C(t)e^{-\Lambda(t)}, \\ n_1(t) &= e^{-\Lambda(t)}\left[n_1(0) + \int_0^t r_2(t')e^{\Lambda(t')}dt'\right]. \end{aligned} \tag{A2}$$

Integrating by parts, the equation is transformed to

$$n_1(t) - \bar{n}_1(t) = e^{-\Lambda(t)}[n_1(0) - \bar{n}_1(0)] - e^{-\Lambda(t)}\int_0^t e^{\Lambda(t')}d\bar{n}_1(t'), \tag{A3}$$

where

$$\bar{n}_1(t) = \frac{r_2(t)}{\lambda(t)} = \frac{1}{1 + e^{\Delta/T(t)}} \tag{A4}$$

is the equilibrium occupation of the state 1 at the temperature $T(t)$.

The above consideration can be readily applied to the case of degenerate levels by the substitution $r_1 \to g_2 r_1$, $r_2 \to g_1 r_2$. In this case, the last expression reads

$$\bar{n}_1 = \frac{1}{1 + \frac{g_2}{g_1}e^{\Delta/T}}.$$

If $\Delta = 0$, $\bar{n}_1 = g_1/(g_1 + g_2)$ is temperature and, consequently, time independent and Eq. (A3) takes a simple form

$$\frac{n_1(t) - \bar{n}_1}{n_1(0) - \bar{n}_1} = e^{-\Lambda(t)}. \tag{A5}$$

The equilibrium population can be excluded to obtain the equation in terms of the population difference,

$$\frac{g_2 n_1(t) - g_1 n_2(t)}{g_2 n_1(0) - g_1 n_2(0)} = e^{-\Lambda(t)}. \tag{A6}$$

[1] A. Fujishima and K. Honda, Nature **238**, 37 (1972).
[2] M. Xu, Y. Gao, E. M. Moreno, M. Kunst, M. Muhler, Y. Wang, H. Idriss, and C. Wöll, Phys. Rev. Lett. **106**, 138302 (2011).
[3] T. Luttrell, S. Halpegamage, J. Tao, A. Kramer, E. Sutter, and M. Batzill, Sci. Rep. **4**, 4043 (2014).
[4] H. Tang, K. Prasad, R. Sanjinés, P. E. Schmid, and F. Lévy, J. Appl. Phys. **75**, 2042 (1994).
[5] K. Tanaka, M. F. Capule, and T. Hisanaga, Chem. Phys. Lett. **187**, 73 (1991).
[6] A. L. Linsebigler, G. Lu, and J. T. Yates, Chem. Rev. **95**, 735 (1995).
[7] X. Chen, L. Liu, P. Y. Yu, and S. S. Mao, Science **331**, 746 (2011).
[8] C. G. Van de Walle and J. Neugebauer, Nature **423**, 626 (2003).
[9] C. G. Van de Walle, Phys. Rev. Lett. **85**, 1012 (2000).
[10] C. Kilic and A. Zunger, Appl. Phys. Lett. **81**, 73 (2002).
[11] D. J. Park, H. H. Nahm, and C. H. Park, J. Korean Phys. Soc. **49**, S473 (2006).
[12] H. H. Nahm and C. H. Park, J. Korean Phys. Soc. **56**, 485 (2010).
[13] C. Sun, Y. Jia, X.-H. Yang, H.-G. Yang, X. Yao, G. Q. M. Lu, A. Selloni, and S. C. Smith, J. Phys. Chem. C **115**, 25590 (2011).

[14]M. Mehta, N. Kodan, S. Kumar, A. Kaushal, L. Mayrhofer, M. Walter, M. Moseler, A. Dey, S. Krishnamurthy, S. Basu, and A. P. Singh, J. Mater. Chem. A **2670** (2016).
[15]E. V. Lavrov, Phys. Status Solidi A **212**, 1494 (2015).
[16]E. V. Lavrov, Phys. Rev. B **93**, 045204 (2016).
[17]G. D. Watkins and J. W. Corbett, Phys. Rev. **121**, 1001 (1961).
[18]M. Stavola, K. Bergman, S. J. Pearton, and J. Lopata, Phys. Rev. Lett. **61**, 2786 (1988).
[19]Y. M. Cheng and M. Stavola, Phys. Rev. Lett. **73**, 3419 (1994).
[20]M. Stavola, Y. M. Cheng, and G. Davies, Phys. Rev. B **54**, 11322 (1996).
[21]M. Stavola, S. J. Pearton, J. Lopata, C. R. Abernathy, and K. Bergman, Phys. Rev. B **39**, 8051 (1989).
[22]D. M. Kozuch, M. Stavola, S. J. Spector, S. J. Pearton, and J. Lopata, Phys. Rev. B **48**, 8751 (1993).
[23]F. Börrnert, E. V. Lavrov, and J. Weber, Phys. Rev. B **75**, 205202 (2007).
[24]E. V. Lavrov, J. Weber, and F. Börrnert, Phys. Rev. B **77**, 155209 (2008).
[25]P. Weiser, Y. Qin, W. Yin, M. Stavola, W. B. Fowler, and L. A. Boatner, Appl. Phys. Lett. **109**, 202105 (2016).
[26]A. J. Hupfer, E. V. Monakhov, B. G. Svensson, I. Chaplygin, and E. V. Lavrov, Sci. Rep. **7**, 17065 (2017).
[27]E. V. Lavrov and J. Weber, Phys. Rev. B **73**, 035208 (2006).
[28]E. V. Lavrov and J. Weber, Phys. Status Solidi B **243**, 2657 (2006).
[29]T. Arlt, M. Bermejo, M. A. Blanco, L. Gerward, J. Z. Jiang, J. Staun Olsen, and J. M. Recio, Phys. Rev. B **61**, 14414 (2000).
[30]L. Gerward and J. Staun Olsen, J. Appl. Crystallogr. **30**, 259 (1997).
[31]H. Eyring, J. Chem. Phys. **3**, 107 (1935).
[32]C. Wert and C. Zener, Phys. Rev. **76**, 1169 (1949).
[33]G. H. Vineyard, J. Phys. Chem. Solids **3**, 121 (1957).